Co-expression network analysis of gene expression profiles of HER2+ breast cancer-associated brain metastasis

FENG YUAN[*], WEI WANG[*] and HONGTAO CHENG

Department of Breast Surgery, Hubei Cancer Hospital, Tongji Medical College, Huazhong University of Science and Technology, Wuhan, Hubei 430079, P.R. China

Abstract. Brain metastasis occurs in ~30% of patients with breast cancer, and patients with human epidermal growth factor receptor 2 (HER2)+ breast cancer have a particularly high frequency of brain metastasis. Weighted gene co-expression network analysis was conducted to identify the hub differentially expressed genes from patients with HER2+ breast cancer between brain metastases and primary tumors. The potential candidate genes were investigated in another set of patient samples to confirm their relevance. The results indicated that a number of pathways altered significantly when breast cancer metastasized to the brain. Cyclophilin A (CypA) and ribosomal protein L17 (RPL17) were overexpressed in breast cancer-associated brain metastases, whereas tumor protein 63 (TP63) and von Willebrand factor A domain-containing 8 (VWA8) were significantly downregulated in breast cancer brain metastases. Furthermore, the expression of CypA and RPL17 in brain metastases were significantly increased compared with that in primary breast tumors, and the expression of TP63 and VWA8 in brain metastases were significantly decreased. This result indicated that the significant differences in expression observed between primary breast tumors and brain metastases were derived from significantly altered systems, including gene modules rather than single genes.

Introduction

Brain metastasis occurs in ~30% of patients with breast cancer (1). Owing to the lack of effective therapeutic treatments, breast cancer brain metastasis can cause significant morbidity, resulting in a poor prognosis. A number of characteristics are associated with the development of primary breast cancer into brain metastases, including being diagnosed at a young age, hormone receptor-negative status, tumors >20 mm in diameter, lymph node invasion, grade 3 and human epidermal growth factor receptor 2 (HER2)+ status (2-4). In another study it has been reported that patients with HER2+ breast cancer have a 2-4-fold increased frequency of brain metastasis (25-37%) compared with patients with HER2- breast cancer (2). The reason HER2 is associated with breast cancer brain metastasis has yet to be determined; however, previous studies identified that the improved extracranial control of disease, inability of treatments to access or be active in the central nervous system (CNS) and the natural predilection for tumor cells to deposit in the CNS may contribute (5,6). Despite the availability of HER2-targeted therapies, e.g., trastuzumab, it is expected that brain metastasis from breast cancer will continue to be a significant clinical problem in the long term.

To address this urgent situation, more biomarkers for the early detection of breast cancer-associated brain metastasis are required. Owing to the development of microarray assays, there has been a significant increase in the data available, broadening and deepening the research concerning biomarkers for breast cancer-associated brain metastasis. Weighted gene co-expression network analysis (WGCNA) is a powerful instrument to identify hub genes in the data from microarray assays. The concept of WGCNA is straightforward: Nodes represent genes and nodes are connected when the corresponding genes are significantly co-expressed across appropriately selected tissue samples (7,8).

In the present study, WGCNA was performed to detect the significant hub genes in a set of samples collected from patients with HER2+ breast cancer, including patients with brain metastasis. Additionally, the potential candidate genes were verified in a set of patient samples using the reverse transcription-quantitative polymerase chain reaction (RT-qPCR).

Materials and methods

Ethics statement. Written informed consent for research was obtained from all patients included in the present study. All

Correspondence to: Dr Hongtao Cheng, Department of Breast Surgery, Hubei Cancer Hospital, Tongji Medical College, Huazhong University of Science and Technology, 116 Zhuodaoquan South Road, Wuhan, Hubei 430079, P.R. China
E-mail: htchengoncologist@gmail.com

[*]Contributed equally

experiments were conducted according to the relevant guidelines and regulations of the Institutional Ethical Review Committee of Hubei Cancer Hospital (Wuhan, China). The present study was approved by the Institutional Ethical Review Committee of Hubei Cancer Hospital.

Data collection. Normalized gene expression data were downloaded from the Gene Expression Omnibus database (www.ncbi.nlm.nih.gov/geo). The dataset GSE43837 was used as a training set to construct expression networks and identify hub genes in the present study. This dataset was based on the microarray platform of Affymetrix Human X3P Array (U133_X3P), which consisted of the expression data of 38 human samples, containing 19 HER2$^+$ human breast cancer-associated brain metastases and 19 HER2$^+$ primary human breast tumors. The gene expression data were based on the RNA microdissection and hybridization technology, as reported previously (9).

Study population. A total of 28 patients between 28 and 65 years old with HER2$^+$ breast cancer treated at the Hubei Cancer Hospital from 1 January 2012 to 31 December 2016 were included in the present study and utilized as the testing set for the confirmation of hub genes determined from the training set. The inclusion criteria for the patients participating in the present study were the following: Primary diagnosis for HER2+ breast cancer with tumours harvested during operation and all patients were diagnosed with brain metastasis at different time points following operation, with the brain being the first site of relapse. Harvested tumors were subsequently stored in liquid nitrogen (25 kpa) at -195.79˚C for long-term storage. In addition, the brain metastasis samples were harvested following diagnosis and kept in liquid nitrogen. The clinical characteristics of the patients included in the present study are indicated in Table I.

Data preprocessing. For each patient included in the training set, when brain metastasis occurred, a value of 1 was assigned; otherwise, a value of 0 was assigned for patients without brain metastasis.

Co-expression network construction. The WGCNA R package software (R version 2.15.3 for Windows; www.r-project.org) was used to perform the analysis. Primarily, the genomic expression information of each patient was associated with brain metastasis. Student's t-test was used to determine the association between gene expression and brain metastasis. The significantly altered genes were selected as primary hub genes. In the following steps, according to the official tutorial for the WGCNA R 2.15.3 package software (www.r-project. org) (10), the automatic block-wise network construction and module detection methods were used to construct co-expression networks. Analysis of network topology was also performed to select the feasible soft-thresholding power. Following detection of the gene modules, the corresponding association with brain metastasis was determined. The relative association of the individual gene with brain metastasis was termed 'gene significance'. This was defined by the absolute value of the association between the gene and brain metastasis. Module membership

Table I. General characteristics of the patients included in the present study for testing the hub genes.

Characteristic	n
Patients in total	28
Sex	
Male	0
Female	28
HER2	
Positive	28
Negative	0
ER	
Positive	16
Negative	12
PR	
Positive	19
Negative	9
AJCC grade	
I	4
II	13
III	11
Lymph metastasis prior to BM	
Positive	17
Negative	11
Chemotherapy prior to BM	
Presence	28
Absence	0
Trastuzumab treatment prior to BM	
Presence	7
Absence	21
Endocrine treatment prior to BM	
Presence	13
Absence	15
Radiation therapy prior to BM	
Presence	26
Absence	2

Median age was 47 years; median time to BM following surgery was 9 months. BM, brain metastasis; AJCC, American Joint Committee on Cancer; HER, human epidermal growth factor receptor 2; ER, estrogen receptor; PR, progesterone receptor; BM, brain metastasis.

was also defined as the association between the module eigengene and the gene expression profile to quantify the significance of the association between the gene profile and the module. The module with the strongest association was further analyzed to locate the genes associated with brain metastasis.

Visualization of the network. Following confirmation of the significantly associated genes of the training set, the network of genes was visualized by integrating the information from the process of network construction into the software of Cytoscape (version 3.4; www.cytoscape.org). Cytoscape is open source

Table II. Primers for the reverse transcription-quantitative polymerase chain reaction.

Gene	Forward (5'-3')	Reverse (5'-3')
TP63	TACAGTACTGCCCTGACCCT	CTCTGGGACATGGTGGATCG
CypA	CCGTGTTCTTCGACATTGCC	TTGTCTGCAAACAGCTCAAAGG
VWA8	GGCTACAACATTGGTCTGGT	ATGCAGAACTGAGAGTGGGC
RPL17	TGGCCCAAAAAGAGTGCTGA	GGCGCATCTTAGGTGCTTTG

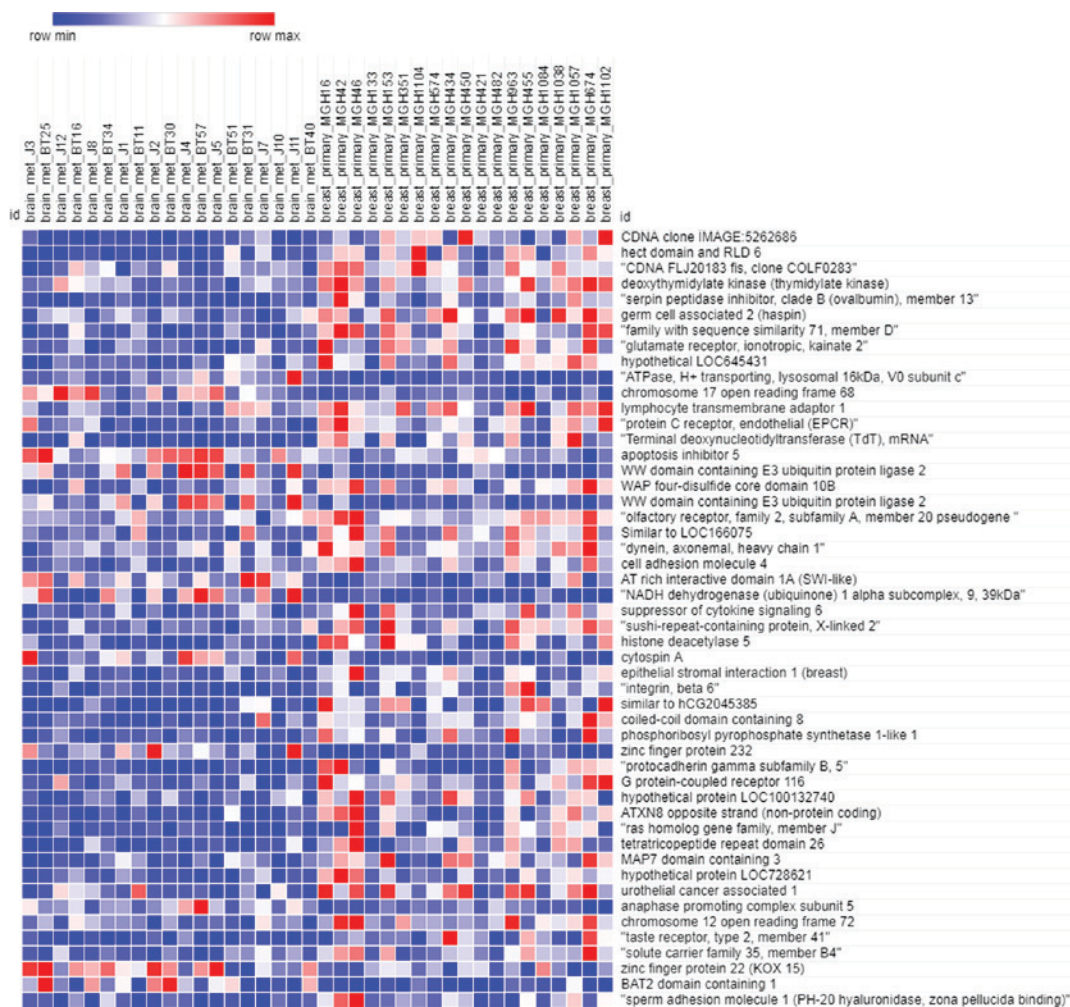TP63, tumor protein p63; RPL17, ribosomal protein L17; CypA, cyclophilin A; VWA8, von Willebrand factor A domain-containing 8.

Figure 1. Heatmap of the overall dataset. Each column represents the corresponding sample of the dataset. Each row represents a gene. The tag title represents the respective tag applied to detect the expression of each gene. As depicted by the color bar, blue represents decreased expression and red represents increased expression.

software for the visualization of molecular interaction networks and biological pathways.

Gene Ontology (GO) and Kyoto Encyclopedia of Genes and Genomes (KEGG) analyses. Subsequently, the relatively significant genes of the networks were added into GO and KEGG (https://david.ncifcrf.gov/) analyses to determine the significant biological processes of the cancer cells. The online analysis tool Database for Annotation, Visualization and Integrated Discovery (david.ncifcrf.gov/tools.jsp) was used to transform the network data in order to conduct GO and KEGG analyses.

RNA extraction and reverse transcription-quantitative polymerase chain reaction (RT-qPCR). Total RNA of the patients in the testing set was extracted from the frozen tissues as previously described (9). For RT-qPCR, a PrimeScript RT Master Mix (Takara Biotechnology Co., Ltd., Dalian, China) was used to synthesize cDNA. SYBR® Real-time PCR Master mix (Toyobo Co., Ltd., Shanghai, China) was used to perform qPCR analyses. The results were normalized with the expression of GAPDH as a reference and quantified using the $2^{-\Delta\Delta Cq}$ method (11). The GAPDH sequence was as follows: Forward, 5'-ACCATCTTCCAGGAGCGAGA-3' and reverse, 5'-GCA
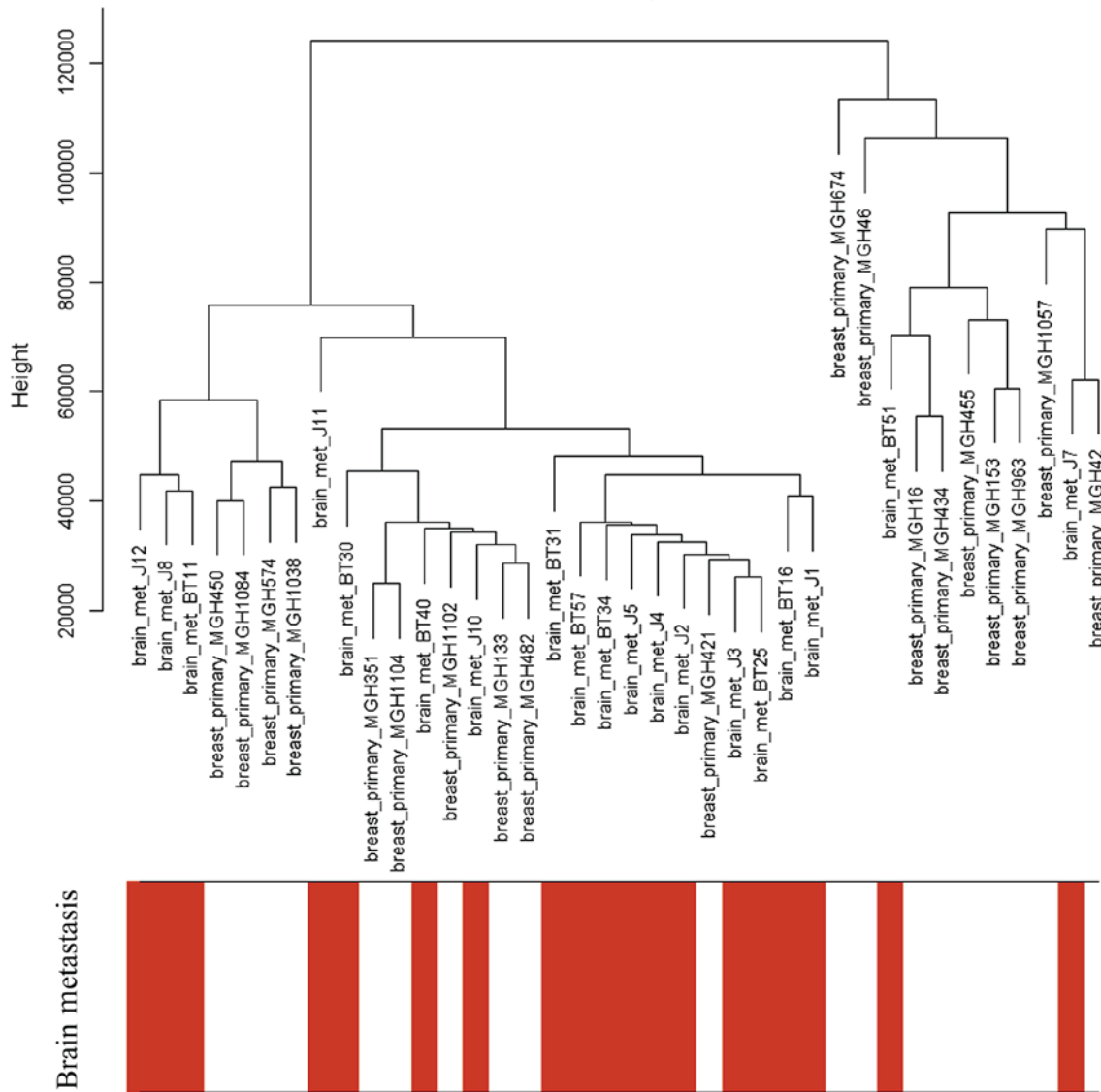
Figure 2. Sample dendrogram and trait heatmap. Samples were clustered according to the expression microarray, and there was no notable outlier; therefore, all the patients were included in the present analysis. White represents 0 (primary tumor) and red represents 1 (brain metastasis).

AATGAGCCCCAGCCTTC-3'. The primers are detailed in Table II. RT-qPCR and data collection were performed using a Bio-Rad CFX Manager 3.0 instrument (Bio-Rad Laboratories, Inc., Hercules, CA, USA). All RT-qPCRs were performed in triplicate. The following thermocycling conditions were used for qPCR: 94˚C for 30 sec; 40 cycles of 60˚C for 30 sec and 72˚C for 30 sec. The data were processed with GraphPad Prism (version 7; GraphPad Software, Inc., La Jolla, CA, USA). P<0.05 was considered to indicate a statistically significant difference.

Results

Construction of the network. As depicted in Fig. 1, the heatmap of the training dataset indicated that the expression profiles in primary breast cancer and brain metastasis were significantly different. There were 4,168 genes included in the training dataset. Owing to the large amount of data, only the expression of the 50 most significant (P<0.05) genes was depicted in the heatmap.

Only the clinical characteristics of brain metastasis were associated with the sample dendrogram, as depicted in Fig. 2. The samples were clustered according to the expression microarray, and there was no notable outlier; therefore, all the patients were included in this analysis.

As depicted in Fig. 3, the power 18 was selected as the lowest power for the scale-free topology for which the fitting index reached 0.90. Different genes were subsequently grouped into modules according to the association of expression (Fig. 4). Each color represented a different module, comprised of gene sets of multiple different genes.

In the clustering tree (dendrogram), each leaf, represented by a short vertical line, corresponded to a gene. Branches of the dendrogram group together to form densely interconnected, highly co-expressed genes. Module identification amounted to the identification of individual branches. Owing to the marked association among the genes inside each module, the modules with similar expression profiles were merged. To quantify the co-expression similarity of entire modules, their eigengenes
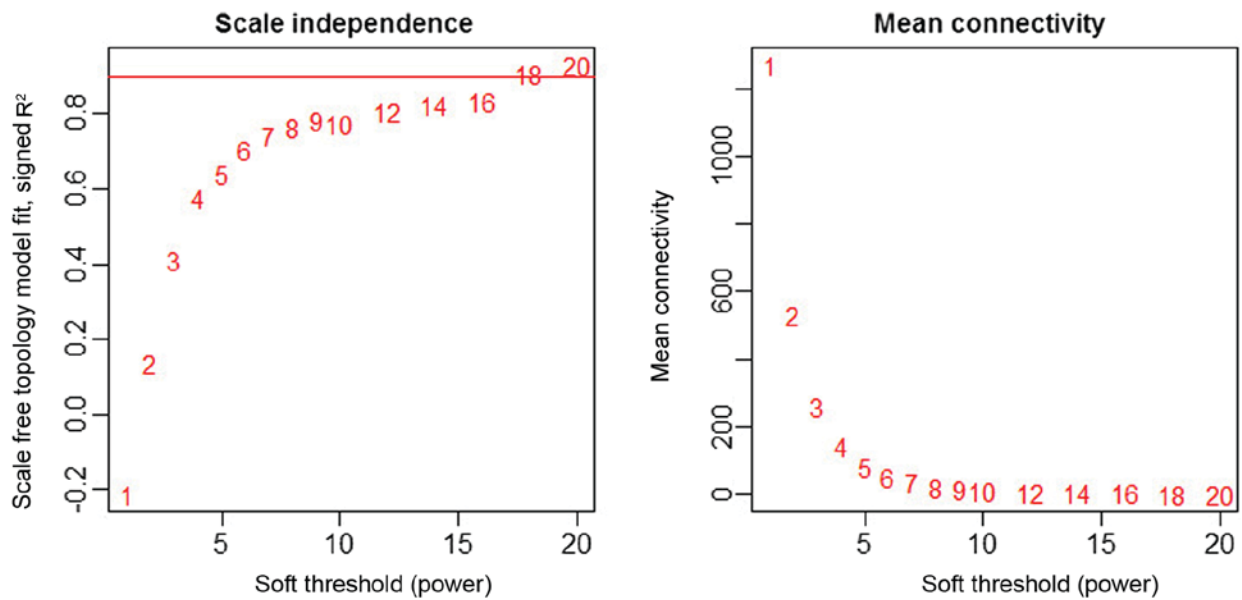
Figure 3. Analysis of network topology for various soft-thresholding powers. Power 18 was selected as the lowest power for the scale-free topology, for which the fitting index reached 0.90.
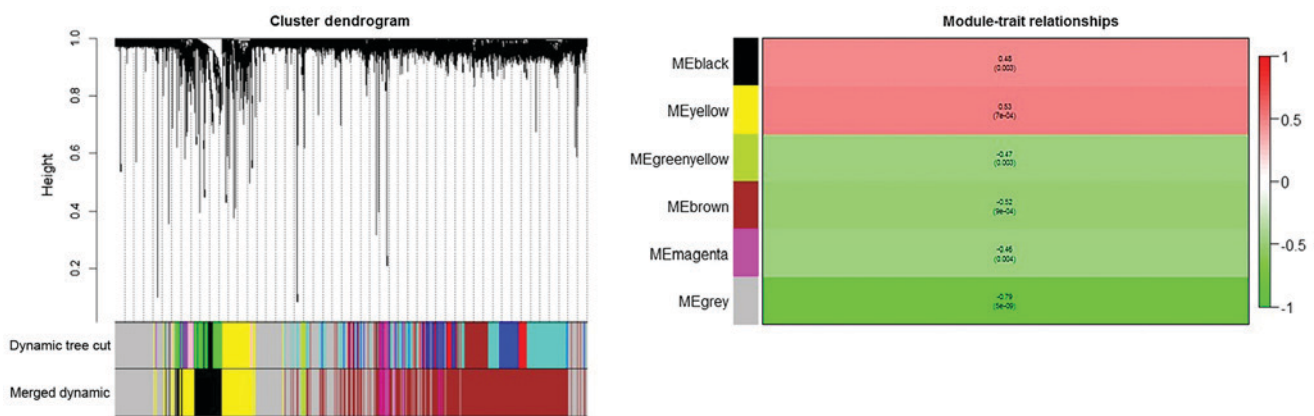

Figure 4. Different genes are grouped into modules according to the association of expression among them. Different colors represent different modules. In the cluster dendrogram, each leaf, represented by a short vertical line, corresponds to a gene. Branches of the dendrogram group together to form densely interconnected highly co-expressed genes. Module identification amounted to the identification of individual branches. Owing to the marked association among the genes inside each module, the modules with similar expression profiles were merged. The modules were associated with brain metastasis according to the overall gene significance inside each module. As depicted by the color bar, the further the value was from 0, the more significant the association was between brain metastasis and the module. Red depicts the positive associations and green depicts the negative associations.

were calculated and were clustered according to their association. The modules were associated with brain metastasis according to the overall gene significance inside each module, and the most significant associations were determined. The further the value was from 0, the more significant the association was between brain metastasis and the module. Red was used to depict the positive associations, and green depicts negative associations. It was indicated that the yellow module had the greatest positive association with breast cancer-associated brain metastasis, whereas the grey module had the lowest negative association.

Figs. 5 and 6 depict the heatmaps of the expression profiles of the yellow module and grey module, respectively. There were 449 genes included in the yellow module and 1,550 genes included in the grey module. Owing to the large amount of data, only the expression of top 50 genes were depicted in the heatmap. According to these heatmaps, the expression profiles in primary breast cancer and brain metastasis were significantly different in each module (P<0.05).

Visualization of the networks. In Figs. 7 and 8, the genes of the yellow module and grey module that had the greatest association with each other were correspondingly integrated into the network. According to the networks, there were two hub genes situated in the center: 211378_39_x_at, representing cyclophilin A (CypA) (also known as peptidylprolyl isomerase A); Hs.82202.2.A1_3p_a_at, representing ribosomal protein L17 (RPL17); g3445483_3p_a_at, representing tumor protein p63 (TP63); and Hs.57787.1.S1_3p_at, representing von Willebrand factor A domain-containing 8 (VWA8).

The expression data of CypA, RPL17, TP63 and VWA8 were extracted from the respective gene modules. As depicted
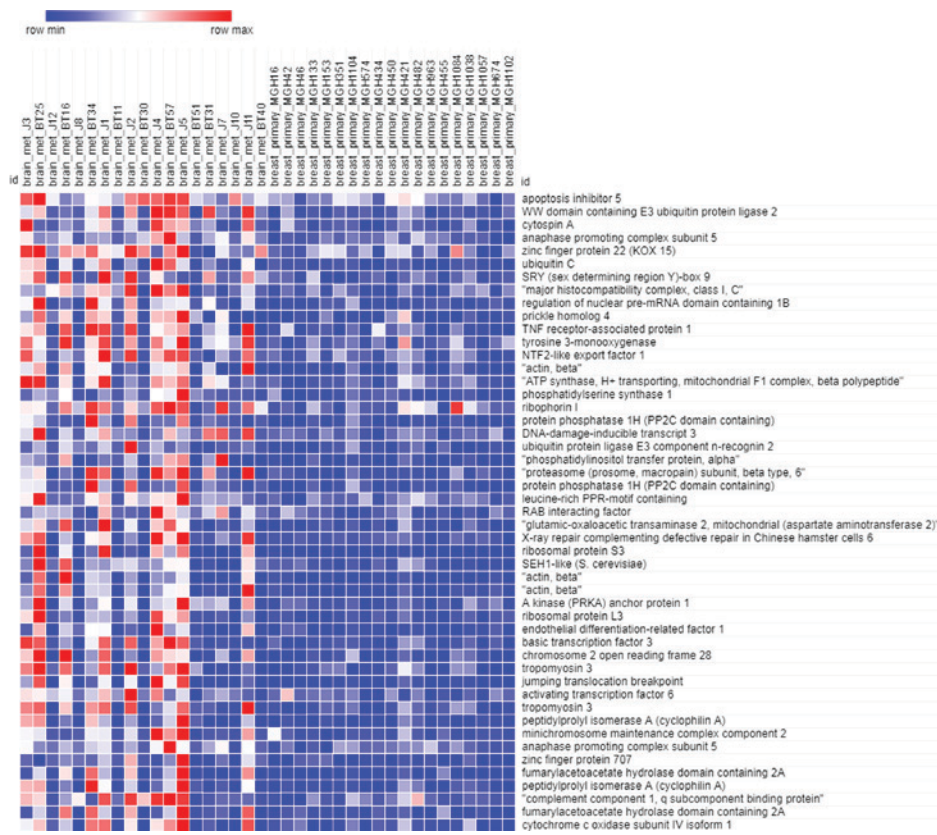
Figure 5. Heatmaps of the expression profile of the yellow module. Each column represents the corresponding sample of the dataset. Each row represents a gene. The tag title represents the respective tag applied to detect the expression of each gene. As depicted by the color bar, blue represents decreased expression and red represents increased expression.
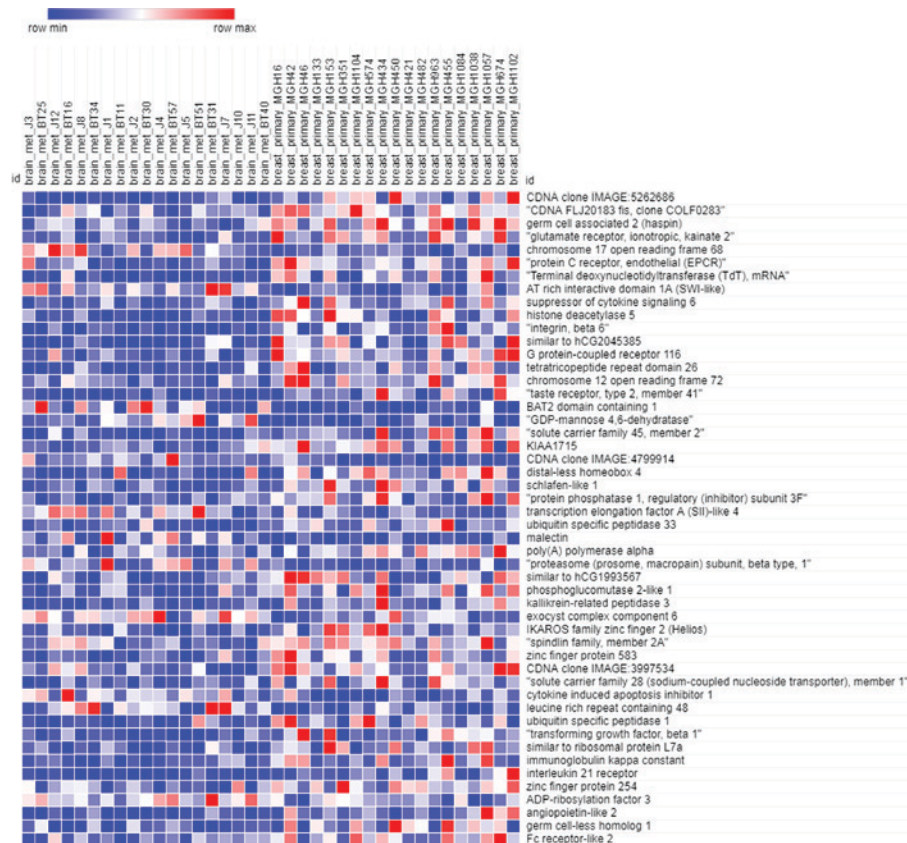

Figure 6. Heatmaps of the expression profile of the grey module. Each column represents the corresponding sample of the dataset. Each row represents a gene. The tag title represents the respective tag applied to detect the expression of each gene. As depicted by the color bar, blue represents decreased expression and red represents increased expression.
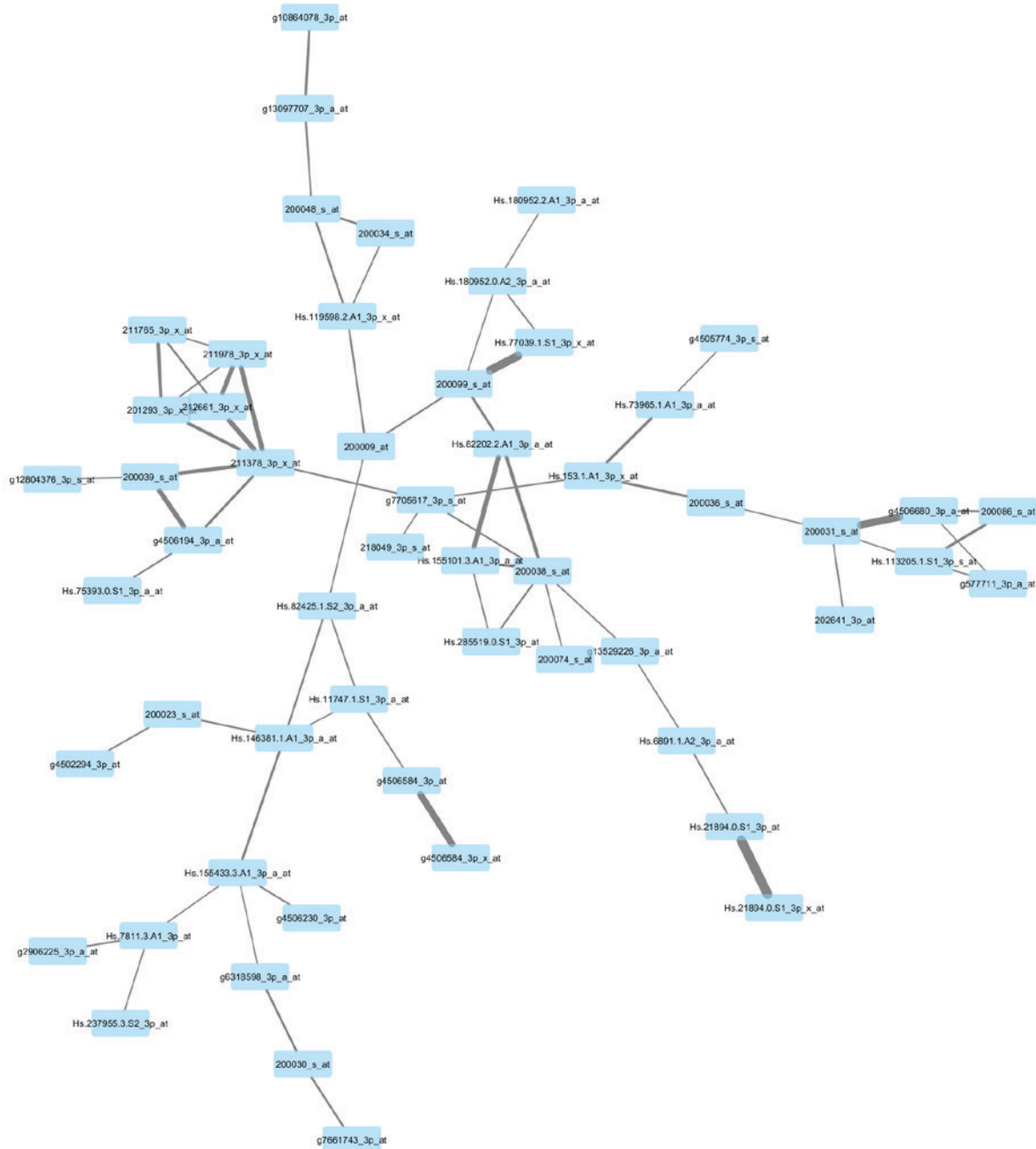
Figure 7. Visualization of the network from the yellow module. Every block represents a gene, and the line between blocks represents the association. The wider the line, the more significant the association.

in Fig. 9, in the training set, CypA and RPL17 were overexpressed in breast cancer-associated brain metastasis, whereas the expression of TP63 and VWA8 was significantly downregulated in breast cancer-associated brain metastasis.

GO and KEGG pathway analysis. Fig. 10 depicts the results of GO and KEGG pathway analysis of the yellow and grey modules, respectively. According to the results, a number of pathways changed significantly when breast cancer metastasized to the brain. For the yellow module, the process of antigen processing and presentation of endogenous peptide antigen was the most significant biological process (BP), the component of the proton-transporting ATP synthase complex was the most significant cell component (CC), the function of

transporter associated with antigen processing binding was the most significant molecular function (MF) and the pathway of base excision repair was the most significant KEGG pathway. For the grey module, the process of regulation of activin receptor signaling pathway was the most significant BP, the component of actin cap was the most significant CC, the function of Toll-like receptor 4 binding was the most significant MF and the pathway of renal cell carcinoma was the most significant KEGG pathway. However, none of the aforementioned genes were included in the significantly influenced pathways.

Hub gene confirmation in patient samples. As depicted in Fig. 11, in the patient samples from the testing set, which
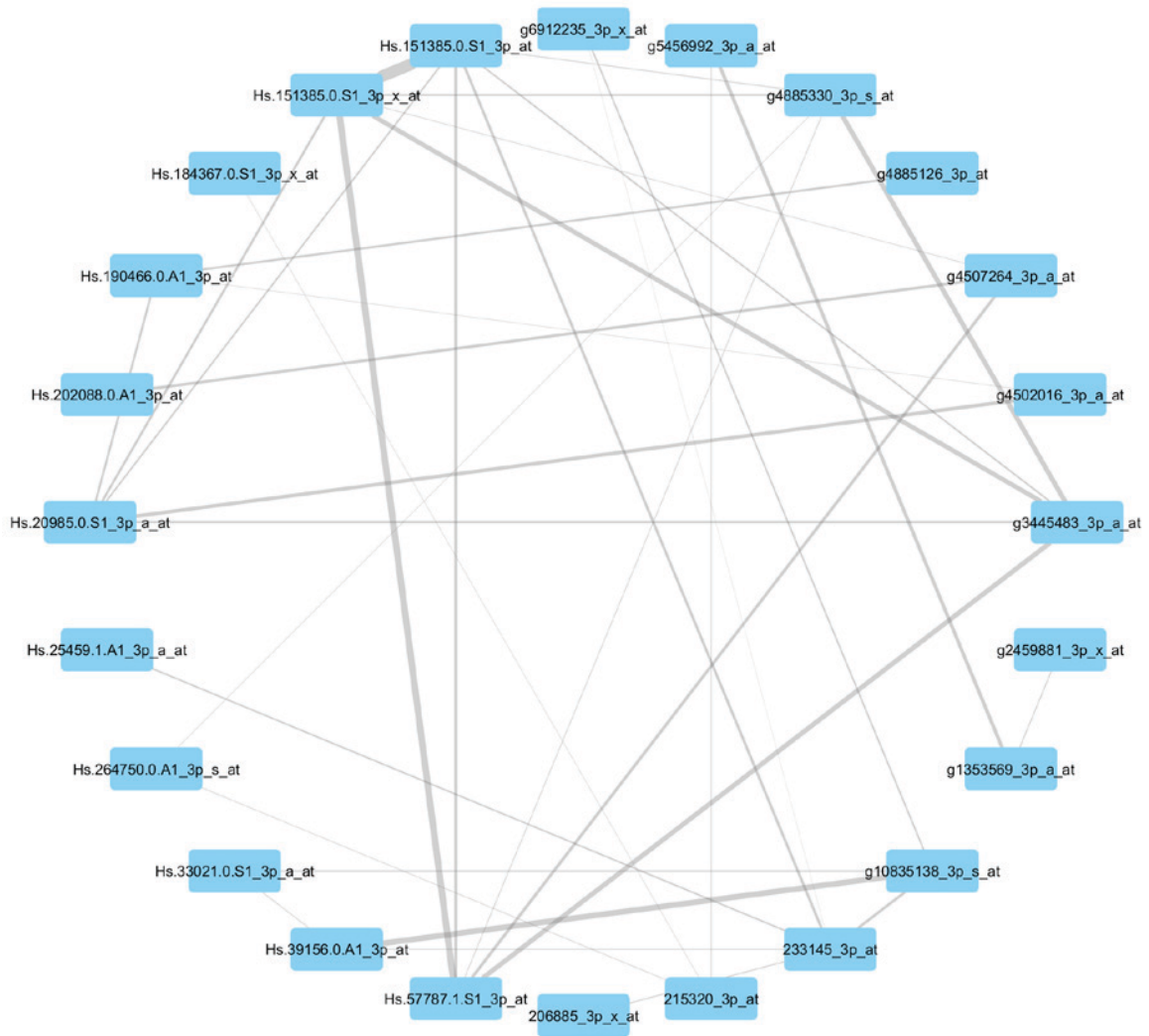
Figure 8. Visualization of the network from the grey module. Every block represents a gene, and the line between blocks represents the association. The wider the line, the more significant the association.
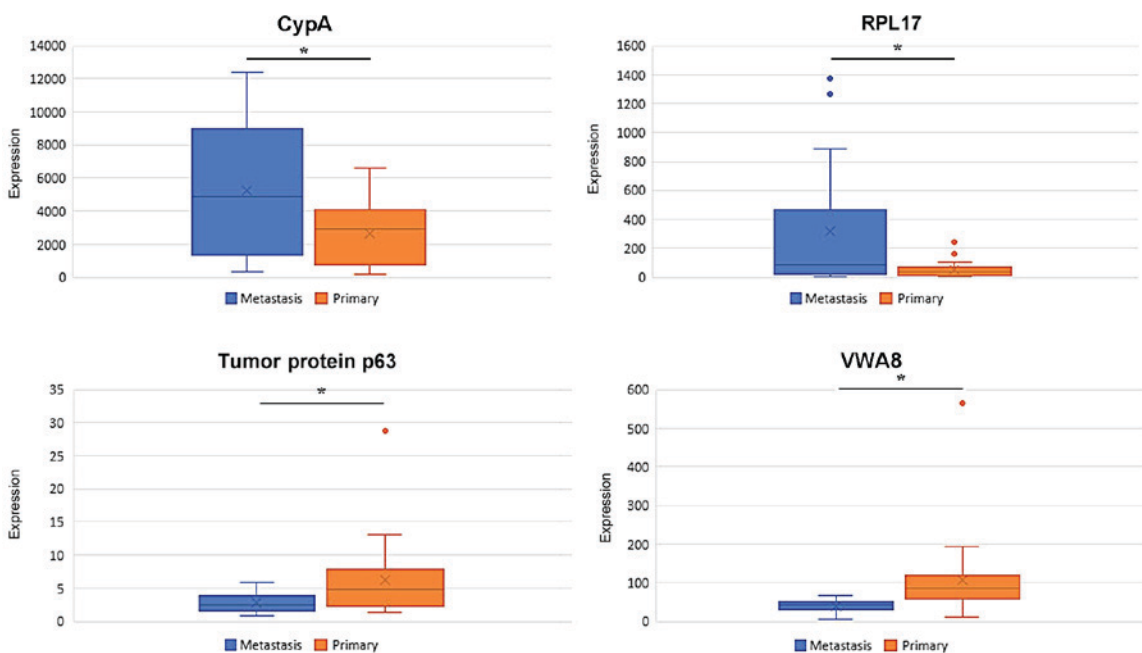

Figure 9. Original expression data of CypA, RPL17, TP63 and VWA8 in the training dataset. *P<0.05. CypA, cyclophilin A; RPL17, ribosomal protein L17; TP63, tumor protein p63; VWA8, von Willebrand factor A domain-containing 8.
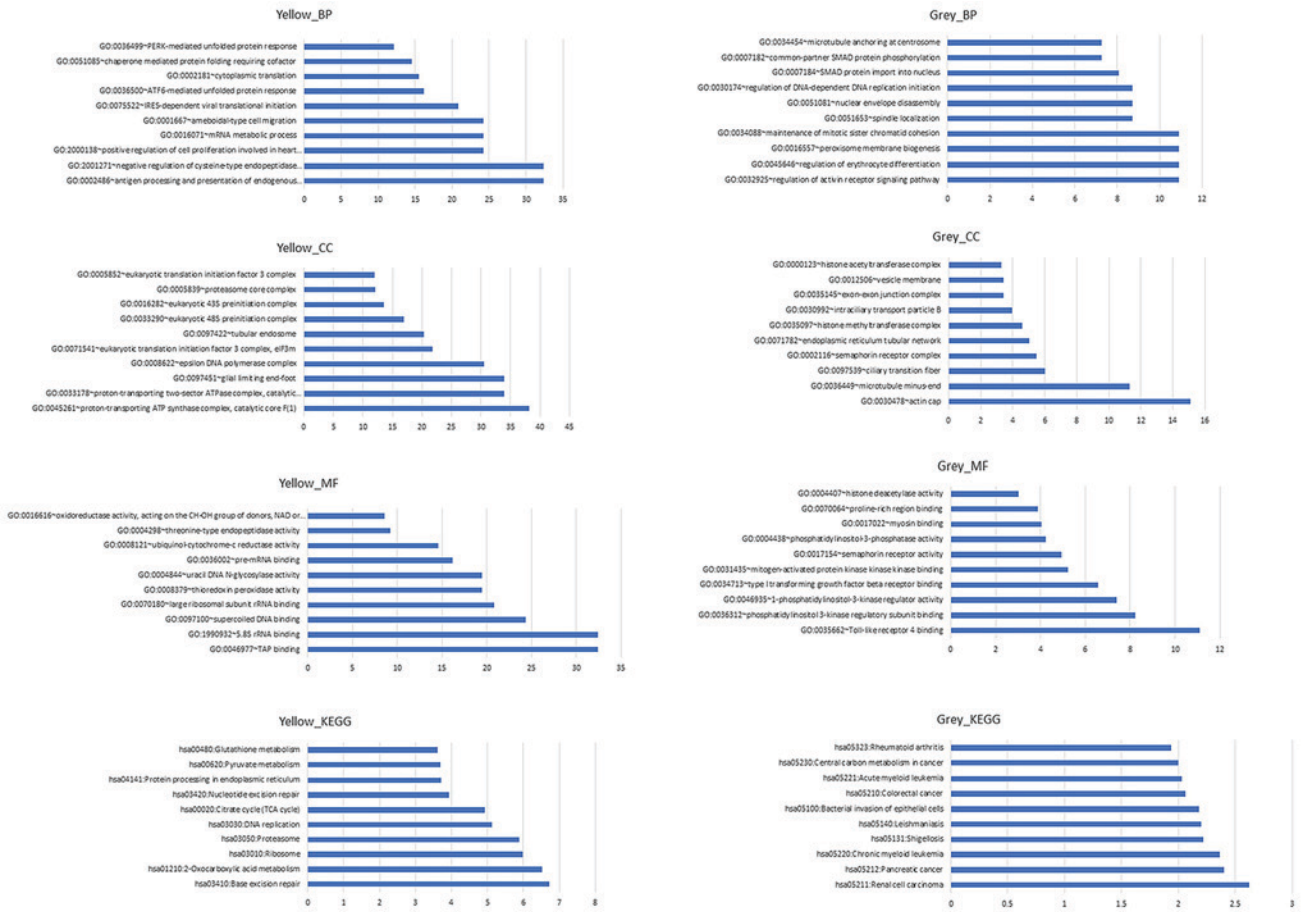
Figure 10. Corresponding results of GO analysis and KEGG pathway analysis for the yellow module and grey module. GO, Gene Ontology; KEGG, Kyoto Encyclopedia of Genes and Genomes; BP, biological process; CC, cell component; MF, molecular function.
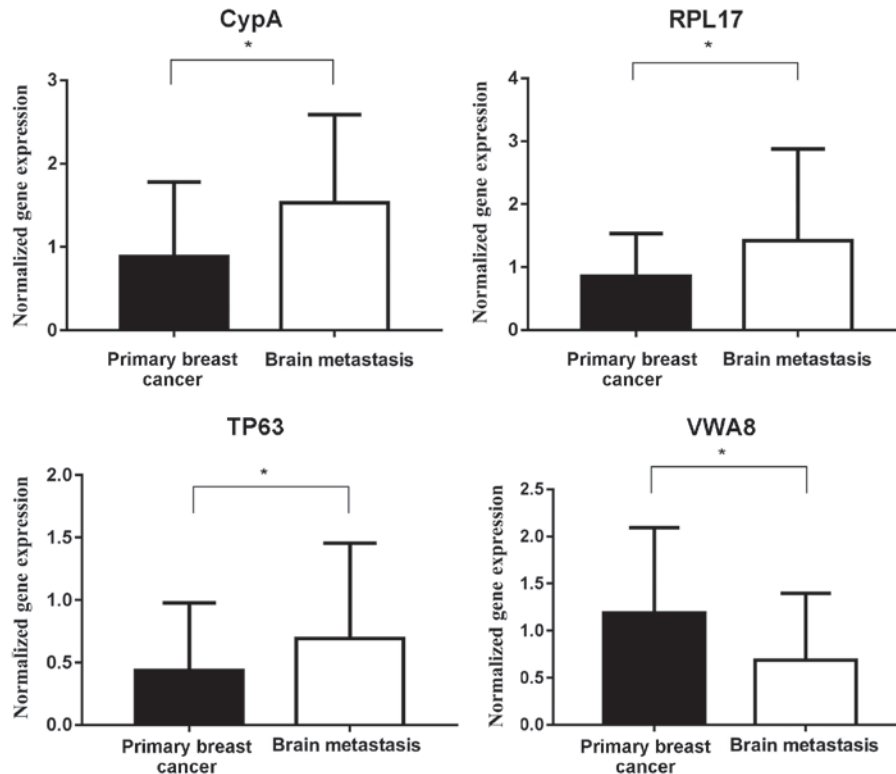

Figure 11. The expression level of CypA, RPL17, TP63 and VWA8 in patients with primary breast tumors compared with brain metastases. *P<0.05. CypA, cyclophilin A; RPL17, ribosomal protein L17; TP63, tumor protein p63; VWA8, von Willebrand factor A domain-containing 8.
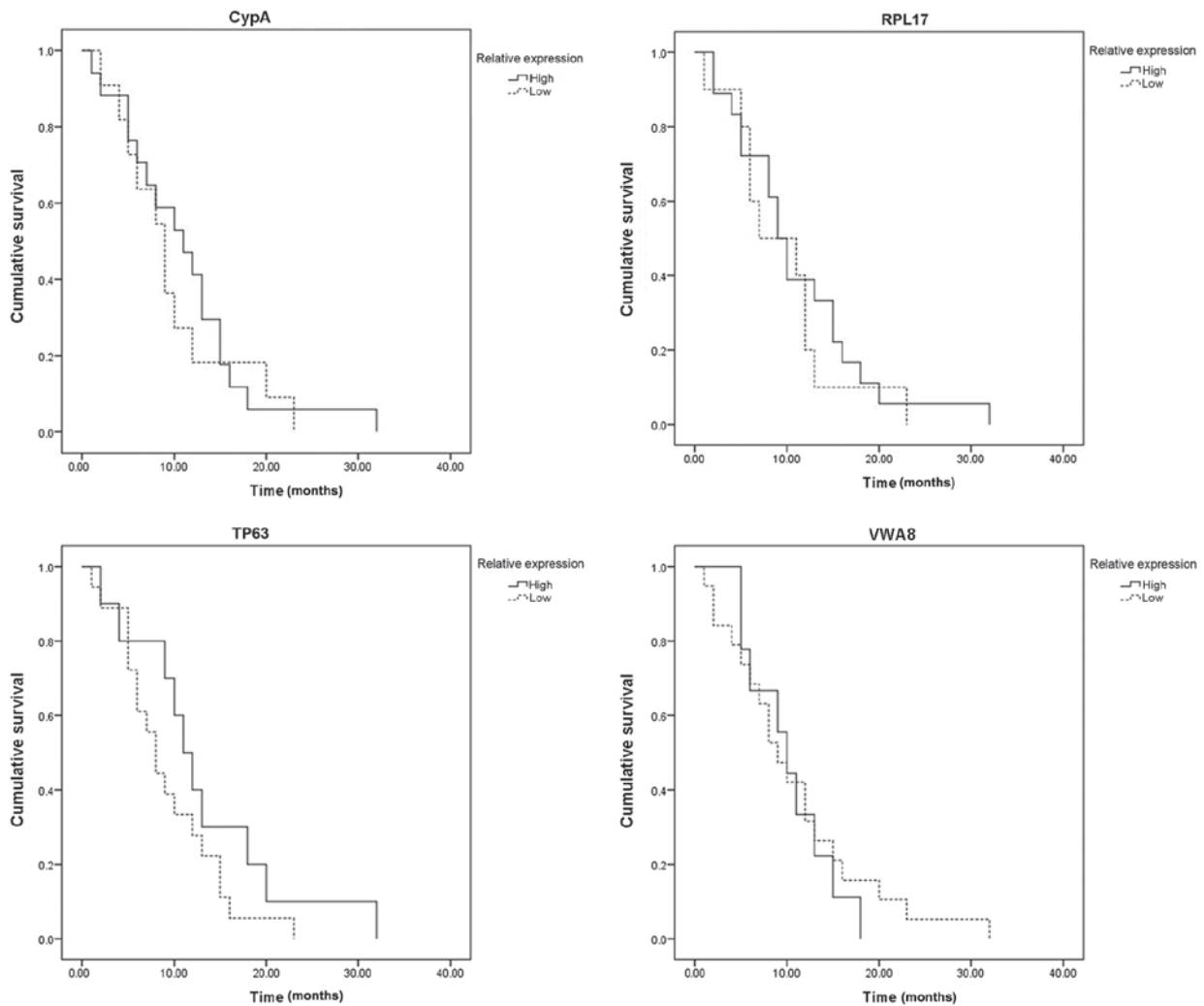
Figure 12. The expression level of CypA, RPL17, TP63 and VWA8 associated with the progression to brain metastasis following surgery for primary breast cancer. P>0.05. CypA, cyclophilin A; RPL17, ribosomal protein L17; TP63, tumor protein p63; VWA8, von Willebrand factor A domain-containing 8.

included all 28 patients, the expression of CypA and RPL17 in brain metastases was significantly increased, compared with in primary breast tumors, and the expression of TP63 and VWA8 in brain metastases was significantly decreased, compared with in primary breast tumors.

Fig. 12 indicated that the expression of the four hub genes was associated with progression to brain metastasis following surgery for primary breast cancer; however, a positive marker associated with brain metastasis-free survival time was not determined.

Discussion

Cyclophilins (Cyps) are proteins that bind to cyclosporin and serve an immunosuppressive role following organ transplantation (12). CypA is one of the 16 family members constituting human Cyps (13). The expression of CypA was reported to be upregulated in a number of malignant tumor types, including small-cell lung cancer (14), pancreatic cancer (15), hepatocellular carcinoma (16) and breast cancer (17). The presence of CypA was considered to promote cellular proliferation and protect those cancer cells against apoptosis or oxidative stress (13). In the present study, the results of the network analysis demonstrated that the upregulated CypA expression was significantly associated with breast cancer-associated brain metastasis in patients with HER2⁺ breast cancer. The identification testing in patient samples also determined that CypA may promote breast cancer cells to metastasize to brain tissue.

RPL17, a member of the L22P family of ribosomal proteins, has been indicated to be located in the cytoplasm (18). Due to the encoded protein sharing an amino acid identity with RPL23 from *Halobacterium marismortui*, the official name of this gene is RPL17 (19). RPL17 could promote multidrug resistance in gastric cancer cells by suppressing drug-induced apoptosis (20,21). In human osteosarcoma, the overexpression of RPL17 may result in stabilization and activation of p53, which serves a pivotal role in suppressing cancer cell proliferation (22). In the network analysis of the present study, the results indicated that the expression of RPL17 was significantly downregulated in primary breast tumors, compared with in metastatic brain tumors. Furthermore, in the patient samples, the expression of RPL17 was more suppressed in primary tumors, compared with brain metastatic neoplasms. The results may indicate that in breast cancer, RPL17 could promote tumor cell invasion and migration.

TP63 is a member of the p53 family, which consists of numerous transcription factors including, p53, p63 and p73 (21), and is reported to be involved in the process of epithelial development and carcinogenesis (23). In normal breast tissue, TP63 expression is restricted to basal/myoepithelial cells, and p63 is essential for mammary gland morphogenesis during embryonic development (24-26). TP63 is highly expressed in a subset of tumors lacking the expression of the estrogen receptor, progesterone receptor and HER2, which is denoted as triple-negative breast cancer (27-29). As aforementioned, patients with HER2^{+} breast cancer have an increased probability of developing brain metastasis, compared with patients without HER2 expression. Orzol *et al* (30) introduced in their research that knocking out TP63 caused breast cancer cells to proliferate at a decreased rate and adhere less tightly, which resulted in an increased rate of migration. In the present study, the network analysis indicated that the expression of TP63 was negatively associated with HER2^{+} breast cancer-associated brain metastasis, which indicated that an increased expression of TP63 was associated with decreased frequency of brain metastasis occurrence. Furthermore, in the patient samples, compared with primary breast tumors, the expression of TP63 in brain metastasis tumors was notably decreased.

The VWA8 gene was originally identified by the Kazusa cDNA project, where it was termed VWA8 (31). Sequence analysis demonstrated that the protein encoded by the VWA8 gene may contain a VWA domain in its C-terminus (31). Data from curated expression analysis of VWA8 in human tissues indicated that VWA8 expression was marked in organs that had high-energy requirements, including organs with a high density of mitochondria (31). The presence of VWA8 exclusively in mitochondria raised the possibility that this protein had a role in metabolic regulation or bioenergetic events (31); however, to date, there is no research concerning its role in malignant tumor types. In the network analysis of the present study, the results indicated that the upregulated expression of VWA8 was negatively associated with breast cancer-associated brain metastasis. Additionally, in the patient samples, the expression of VWA8 in primary breast tumors was notably increased, compared with the metastatic brain tumors.

Furthermore, none of the four genes aforementioned were associated with brain metastasis-free survival time. This may be attributable to the following reasons. First, the quantity of patients with HER2^{+} brain metastasis was too small. At present, there are only 28 patients with HER2^{+} breast cancer-associated brain metastasis that could be included in the analysis. Secondly, the treatments the patients received following surgery may influence the occurrence of brain metastasis. According to Romond *et al* (32), the application of trastuzumab for patients with HER2^{+} may significantly delay the occurrence of brain metastasis, while its effectiveness remains unclear. Thirdly, the different grades of breast cancer prior to surgery and early lymph-node metastasis may also influence the occurrence of brain metastasis (33). To determine how the actual mechanism regulates the occurrence of breast cancer-associated brain metastasis, further clinical and basic research is required.

Primarily, the results of the network analysis in the present study were confirmed in the patient samples to a certain extent. A number of novel target genes were identified, which may provide a novel foundation for targeted therapeutic treatments of HER2^{+} breast cancer-associated brain metastasis. Although numerous genes that function together and constitute networks were determined, the core hub genes were not identified as the most significantly changed genes, and they did not serve pivotal functions in the most significantly influenced signaling pathways. However, as aforementioned, the significant differences observed between primary breast tumors and brain metastatic neoplasms were derived from significantly altered systems, specifically, gene modules rather than single molecules.

Acknowledgements

Funding

Availability of data and materials

The datasets (GSE43837) generated and analyzed during the study are available from the corresponding author, on reasonable request.

Authors' contributions

FY and WW wrote the manuscript and conducted related experiments and data analysis. HC designed the study and discussed the findings. All authors have read and approved the manuscript.

Ethics approval and consent to participate

Written informed consent for research was obtained from all patients included in the present study. All experiments were conducted according to the relevant guidelines and regulations of the Institutional Ethical Review Committee of Hubei Cancer Hospital (Wuhan, China). The present study was approved by the Institutional Ethical Review Committee of Hubei Cancer Hospital.

Patient consent for publication

Not applicable.

Competing interests

The authors declare that they have no competing interests.

References

1. Tsukada Y, Fouad A, Pickren JW and Lane WW: Central nervous system metastasis from breast carcinoma. Autopsy study. Cancer 52: 2349-2354, 1983.
2. Kennecke H, Yerushalmi R, Woods R, Cheang MC, Voduc D, Speers CH, Nielsen TO and Gelmon K: Metastatic behavior of breast cancer subtypes. J Clin Oncol 28: 3271-3277, 2010.
3. Aversa C, Rossi V, Geuna E, Martinello R, Milani A, Redana S, Valabrega G, Aglietta M and Montemurro F: Metastatic breast cancer subtypes and central nervous system metastases. Breast 23: 623-628, 2014.

4. Soni A, Ren Z, Hameed O, Chanda D, Morgan CJ, Siegal GP and Wei S: Breast cancer subtypes predispose the site of distant metastases. Am J Clin Pathol 143: 471-478, 2015.

5. Brufsky AM, Mayer M, Rugo HS, Kaufman PA, Tan-Chiu E, Tripathy D, Tudor IC, Wang LI, Brammer MG, Shing M, *et al*: Central nervous system metastases in patients with HER2-positive metastatic breast cancer: Incidence, treatment, and survival in patients from registHER. Clin Cancer Res 17: 4834-4843, 2011.

6. Shen Q, Sahin AA, Hess KR, Suki D, Aldape KD, Sawaya R and Ibrahim NK: Breast cancer with brain metastases: Clinicopathologic features, survival, and paired biomarker analysis. Oncologist 20: 466-473, 2015.

7. Zhang B and Horvath S: A general framework for weighted gene co-expression network analysis. Stat Appl Genet Mol Biol 4: Article17, 2005.

8. Horvath S, Zhang B, Carlson M, Lu KV, Zhu S, Felciano RM, Laurance MF, Zhao W, Qi S, Chen Z, *et al*: Analysis of oncogenic signaling networks in glioblastoma identifies ASPM as a molecular target. Proc Natl Acad Sci USA 103: 17402-17407, 2006.

9. Chang L, Qi H, Xiao Y, Li C, Wang Y, Guo T, Liu Z and Liu Q: Integrated analysis of noncoding RNAs and mRNAs reveals their potential roles in the biological activities of the growth hormone receptor. Growth Horm IGF Res 29: 11-20, 2016.

10. Langfelder P and Horvath S: WGCNA: An R package for weighted correlation network analysis. BMC Bioinformatics 9: 559, 2008.

11. Livak KJ and Schmittgen TD: Analysis of relative gene expression data using real-time quantitative PCR and the 2(-Delta Delta C(T)) method. Methods 25: 402-408, 2001.

12. Lee J: Role of cyclophilin a during oncogenesis. Arch Pharm Res 33: 181-187, 2010.

13. Zheng J, Koblinski JE, Dutson LV, Feeney YB and Clevenger CV: Prolyl isomerase cyclophilin A regulation of Janus-activated kinase 2 and the progression of human breast cancer. Cancer Res 68: 7769-7778, 2008.

14. Campa MJ, Wang MZ, Howard B, Fitzgerald MC and Patz EF Jr: Protein expression profiling identifies macrophage migration inhibitory factor and cyclophilin A as potential molecular targets in non-small cell lung cancer. Cancer Res 63: 1652-1656, 2003.

15. Cecconi D, Astner H, Donadelli M, Palmieri M, Missiaglia E, Hamdan M, Scarpa A and Righetti PG: Proteomic analysis of pancreatic ductal carcinoma cells treated with 5-aza-2'-deoxycytidine. Electrophoresis 24: 4291-4303, 2003.

16. Corton JC, Moreno ES, Merritt A, Bocos C and Cattley RC: Cloning genes responsive to a hepatocarcinogenic peroxisome proliferator chemical reveals novel targets of regulation. Cancer Lett 134: 61-71, 1998.

17. Chevalier F, Depagne J, Hem S, Chevillard S, Bensimon J, Bertrand P and Lebeau J: Accumulation of cyclophilin A isoforms in conditioned medium of irradiated breast cancer cells. Proteomics 12: 1756-1766, 2012.

18. Kenmochi N, Kawaguchi T, Rozen S, Davis E, Goodman N, Hudson TJ, Tanaka T and Page DC: A map of 75 human ribosomal protein genes. Genome Res 8: 509-523, 1998.

19. Mager DL and Freeman JD: A human gene related to the ribosomal protein L23 gene of Halobacterium marismortui. Nucleic Acids Res 18: 5301, 1990.

20. Shi Y, Zhai H, Wang X, Han Z, Liu C, Lan M, Du J, Guo C, Zhang Y, Wu K and Fan D: Ribosomal proteins S13 and L23 promote multidrug resistance in gastric cancer cells by suppressing drug-induced apoptosis. Exp Cell Res 296: 337-346, 2004.

21. Pflaum J, Schlosser S and Müller M: p53 family and cellular stress responses cancer. Front Oncol 4: 285, 2014.

22. Jin A, Itahana K, O'Keefe K and Zhang Y: Inhibition of HDM2 and activation of p53 by ribosomal protein L23. Mol Cell Biol 24: 7669-7680, 2004.

23. Yang A, Kaghad M, Wang Y, Gillett E, Fleming MD, Dötsch V, Andrews NC, Caput D and McKeon F: p63, a p53 homolog at 3q27-29, encodes multiple products with transactivating, death-inducing, and dominant-negative activities. Mol Cell 2: 305-316, 1998.

24. Batistatou A, Stefanou D, Arkoumani E and Agnantis NJ: The usefulness of p63 as a marker of breast myoepithelial cells. In Vivo 17: 573-576, 2003.

25. Barbareschi M, Pecciarini L, Cangi MG, Macrì E, Rizzo A, Viale G and Doglioni C: p63, a p53 homologue, is a selective nuclear marker of myoepithelial cells of the human breast. Am J Surg Pathol 25: 1054-1060, 2001.

26. Nylander K, Vojtesek B, Nenutil R, Lindgren B, Roos G, Zhanxiang W, Sjöström B, Dahlqvist A and Coates PJ: Differential expression of p63 isoforms in normal tissues and neoplastic cells. J Pathol 198: 417-427, 2002.

27. Leong CO, Vidnovic N, DeYoung MP, Sgroi D and Ellisen LW: The p63/p73 network mediates chemosensitivity to cisplatin in a biologically defined subset of primary breast cancers. J Clin Invest 117: 1370-1380, 2007.

28. Koker MM and Kleer CG: p63 expression in breast cancer-a highly sensitive and specific marker of metoplastic carcinoma. Am J Surg Pathol 28: 1506-1512, 2004.

29. Du Z, Li J, Wang L, Bian C, Wang Q, Liao L, Dou X, Bian X and Zhao RC: Overexpression of Delta Np63 alpha induces a stem cell phenotype in MCF7 breast carcinoma cell line through the Notch pathway. Cancer Sci 101: 2417-2424, 2010.

30. Orzol P, Nekulova M, Holcakova J, Muller P, Votesek B and Coates PJ: ΔNp63 regulates cell proliferation, differentiation, adhesion, and migration in the BL2 subtype of basal-like breast cancer. Tumour Biol 37: 10133-10140, 2016.

31. Luo M, Mengos AE, Ma W, Finlayson J, Bustos RZ, Xiao Zhu Y, Shi CX, Stubblefield TM, Willis WT and Mandarino LJ: Characterization of the novel protein KIAA0564 (Von Willebrand Domain-containing Protein 8). Biochem Biophys Res Commun 487: 545-551, 2017.

32. Romond EH, Jeong JH, Rastogi P, Swain SM, Geyer CE Jr, Ewer MS, Rathi V, Fehrenbacher L, Brufsky A, Azar CA, *et al*: Seven-year follow-up assessment of cardiac function in NSABP B-31, a randomized trial comparing doxorubicin and cyclophosphamide followed by paclitaxel (ACP) with ACP plus trastuzumab as adjuvant therapy for patients with node-positive, human epidermal growth factor receptor 2-positive breast cancer. J Clin Oncol 30: 3792-3799, 2012.

33. Anders CK, Deal AM, Miller CR, Khorram C, Meng H, Burrows E, Livasy C, Fritchie K, Ewend MG, Perou CM and Carey LA: The prognostic contribution of clinical Breast cancer subtype, age, and race among patients with breast cancer brain metastases. Cancer 117: 1602-1611, 2011.